

## Crystallization behaviour and magnetic properties of sodium-silicate glasses containing iron and manganese oxide

<sup>1\*</sup>Ruzha Harizanova, <sup>1</sup>Ivailo Gugov, <sup>2</sup>Christian Rüssel

<sup>1</sup>University of Chemical Technology and Metallurgy, 8 Kl. Ohridski Blvd., 1756 Sofia, Bulgaria

<sup>2</sup>Institut für Glaschemie "Otto-Schott-Institut", Friedrich-Schiller-Universität, Fraunhoferstr. 6, 07743 Jena, Germany

Received: January 24, 2012; accepted: March 5, 2012

**Abstract.** Oxide glasses and nanocrystalline glass-ceramics, containing large amounts of transition metal ions, exhibit novel and unusual electrical and magnetic properties and find various applications in magnetorheology, electronics, magnetic resonance imaging and sensor technology. The present work is dedicated to the study of the crystallization behaviour, phase formation and the resulting magnetic properties of the synthesized products in the system  $\text{Na}_2\text{O}/\text{MnO}/\text{SiO}_2/\text{Fe}_2\text{O}_3$ . Two glasses with 15 mol%  $\text{Fe}_2\text{O}_3$ -concentration and different MnO concentrations are prepared by melting under oxidizing or reducing conditions. Further, the glasses are annealed by applying different time/temperature programs in order to precipitate nano-scale magnetic crystals. The phase composition and microstructure of the glass-ceramics are studied by X-ray diffraction and electron microscopy. The obtained data are used to reveal the crystallization kinetics. The magnetic properties of the selected samples, measured on a vibrating sample magnetometer, vary from para- to superparamagnetic.

**Keywords:** iron oxide and manganese oxide, crystallization kinetics, nano-scale materials, magnetic properties.

### 1. INTRODUCTION

There are numerous reports on the synthesis and application of oxide glasses containing 3d-transition metal ions [1-14]. These glasses and the corresponding glass-ceramics have interesting and promising electrical and magnetic properties especially if nanocrystals are formed by appropriate heat treatment [15, 16] and find applications as components of ferrofluids in electronics, as solder materials or in magnetorheology. Depending on the phase composition, size and volume fraction of the magnetic particles, the obtained crystals can be used as components of contrast agents in magnetic resonance imaging and in biomagnetic sensors for the detection of different chemical and biochemical substances [17, 18]. Many authors report the synthesis of nanosized magnetic crystals by means of wet chemical routes, i.e. by precipitation of magnetite ( $\text{Fe}_3\text{O}_4$ ) [19-22] but also of  $\text{Co}_3\text{O}_4$  and  $\text{MnFe}_2\text{O}_4$  [22, 23] from aqueous solutions. Another preparation route is the controlled crystallization of glasses containing relatively large amounts of transition metal ions which, however, results in higher tendency for spontaneous crystallization [2, 7, 24-28]. The spontaneous crystallization can be suppressed or even avoided by either adjusting the

glass composition (decreasing the transition metal concentration) or increasing the cooling rate [10, 11, 25]. Thermal annealing of the obtained glasses enables the precipitation of nanosized ferrimagnetic or superparamagnetic particles with tailored size-distribution [10, 11]. In literature, the effect of iron oxides combined with a second transition metal oxide, on the phase composition and microstructure of glassy materials, synthesized by conventional melting techniques, is already reported [7, 25], but attempts to precipitate nanoscale crystals in such complex systems are scarcely performed.

This paper presents a study on the precipitation of nanosized spinel phases from glasses in the system  $\text{Na}_2\text{O}/\text{MnO}/\text{SiO}_2/\text{Fe}_2\text{O}_3$  by using a conventional glass-melting technique and subsequent thermal annealing. Vibration magnetometry permits to determine the magnetic properties of the obtained glass-ceramic materials.

### 2. EXPERIMENTAL

Within the system  $\text{Na}_2\text{O}/\text{MnO}/\text{SiO}_2/\text{Fe}_2\text{O}_3$  two glasses with the following compositions, given in mol%, were prepared:

- glass A:  $13.6\text{Na}_2\text{O}/8.5\text{MnO}/62.9\text{SiO}_2/15.0\text{Fe}_2\text{O}_3$ - $\delta$  (reduced by using  $\text{FeC}_2\text{O}_4 \cdot 2\text{H}_2\text{O}$  as raw material).
- glass B:  $16\text{Na}_2\text{O}/10\text{MnO}/59\text{SiO}_2/15\text{Fe}_2\text{O}_3$  ( $\text{Fe}_2\text{O}_3$  used as raw material).

The samples prepared using  $\text{FeC}_2\text{O}_4$  as raw material are further denoted as "reduced", while

\* To whom all correspondence should be sent:  
e-mail: ruza\_harizanova@yahoo.com

samples melted using  $\text{Fe}_2\text{O}_3$  are designated as “oxidized”. Reagent grade raw materials:  $\text{Na}_2\text{CO}_3$ ,  $\text{MnCO}_3$ ,  $\text{SiO}_2$ ,  $\text{Fe}_2\text{O}_3$  or  $\text{FeC}_2\text{O}_4 \cdot 2\text{H}_2\text{O}$  are used for the preparation of the glasses. The batches (100 g) are homogenized and melted in  $\text{SiO}_2$ -crucibles using a  $\text{MoSi}_2$ -furnace at melting temperatures in the range from 1400 to 1450°C (kept for 1.5 h in air). The melts are cast into a pre-heated graphite mould, transferred to a muffle furnace and kept at 480°C for 10 min. Then, the furnace is switched off and the samples allowed to cool down to room temperature. Further, the glasses A and B are annealed at temperatures in the range from 510 to 700°C, according to the determined  $T_g$ -values, for times from 10 min to 100 h in order to precipitate in them nanocrystalline phase containing 3d-metals. The heating rate from room temperature to the desired annealing temperature was always 10K/min. The annealing temperatures were always clearly above the glass transition temperatures:  $T_g = 490^\circ\text{C}$  for glass A and  $T_g = 494^\circ\text{C}$  for glass B, [25]. The phase compositions are determined by X-ray diffraction (XRD: Siemens, D 5000), using  $\text{Cu}_{K\alpha}$ -radiation; the  $2\theta$ -values were in the range from 10 to 60°. The obtained microstructures are studied by scanning electron microscopy (SEM: JEOL 7001F), the samples are cut, polished and coated with carbon. Secondary (SE), as well as backscattered electrons (BSE) are used for imaging. The magnetic measurements are performed on a vibrating sample magnetometer.

### 3. RESULTS AND DISCUSSION

#### 3.1 Results

Information about the characteristic temperatures and microstructure of glasses A and B is already given in [25]. After annealing of glasses A and B, they are examined by X-ray diffraction and the results are shown in Fig. 1a for the crystallized samples A and in Fig. 1b – for the samples of type B. It is seen from the XRD patterns that the annealing at 550°C for times up to 24 h results in formation of only one crystalline phase in both glasses A and B. The X-ray reflexes of this phase are similar to the reflexes of the phases  $(\text{Mn}_{0.6}, \text{Fe}_{0.4})(\text{Mn}_{0.4}, \text{Fe}_{1.6})\text{O}_4$  (JCPDS 88–1965) and  $\text{Fe}_3\text{O}_4$  (JCPDS 87–2334). However, the relatively broad peaks and the proximity of the main reflexes of the two phases (difference in main peak positions  $\sim 0.7^\circ$ ), do not allow an exact determination of the chemical composition of the formed crystals only by means of XRD. Possibly, the precipitated phase is a solid solution of a mixed spinel type  $(\text{Fe}^{2+}, \text{Mn}^{2+})(\text{Fe}^{3+}, \text{Mn}^{3+})_2\text{O}_4$ .

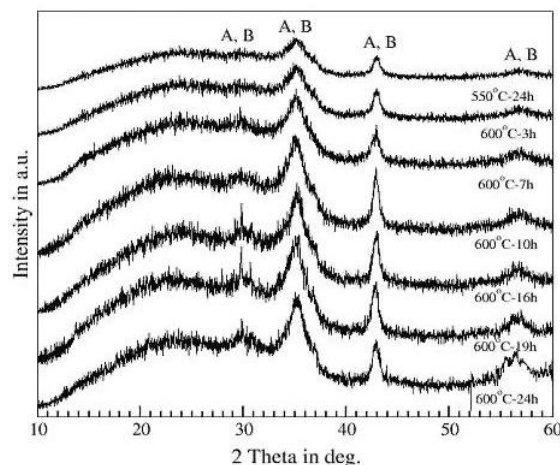


**Fig. 1a** XRD-patterns of samples A annealed at 550 and 600°C for different times- formation of mixed crystals  $\text{MnFe}_2\text{O}_4$  (A) and  $\text{Fe}_3\text{O}_4$  (B)

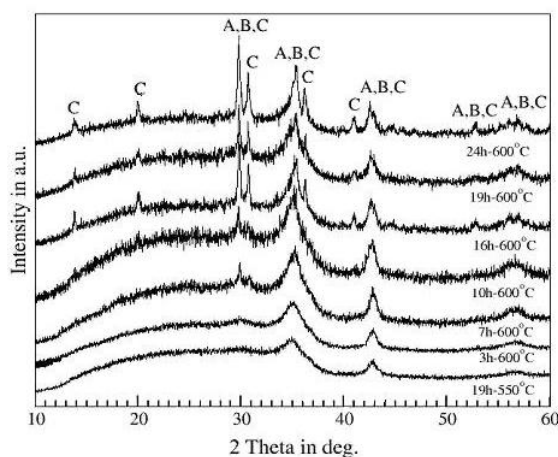


**Fig. 1b** XRD-patterns of samples B, annealed at 550 and 600°C for different times – formation of mixed crystals  $\text{MnFe}_2\text{O}_4$  (A) and  $\text{Fe}_3\text{O}_4$  (B), as well as of  $\text{NaFe}(\text{SiO}_3)_2$  (C)

The observation of one morphological type of crystals is also done while examining the annealed at 550°C samples A by scanning electron microscopy – see Fig. 2a. The average size of the formed spinel crystals is about 50 nm for 3h annealing time, as shown in Fig. 2b (see insert). Similar results are obtained from the SEM micrographs (not shown) of glasses B heat treated at 550°C.

The heat treatment of glasses A and B at 600 °C leads to the formation of two types of crystals: nanosized spinel crystals and micron-sized elongated crystals. This is seen on Fig. 3 for sample A and on Figs. 4a and 4b for sample B. The second crystalline phase is attributed to aegirine,  $\text{NaFe}(\text{SiO}_3)_2$  (JCPDS 34-0185), as shown in Fig. 1b. The average sizes of the formed nanocrystals for the glasses A, annealed at 550°C for times from 40 min to 24 h, are studied in order to investigate the kinetics of crystallization.

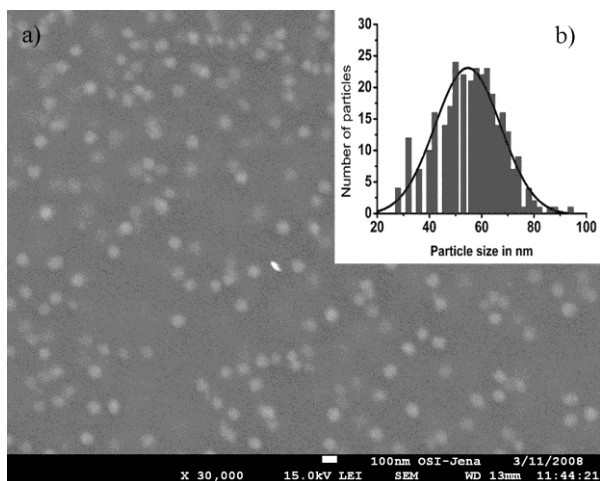


**Fig. 2:** (a) SEM (SE) image of C-covered sample A, annealed for 3 h at 550°C – uniform distribution of the nanosized (Fe, Mn)-based crystals; (b) Gauss-fitted chart with the size distribution of the nanocrystals, precipitated in sample A, annealed for 3 h at 550°C – maximum centred at about  $54 \pm 1$  nm

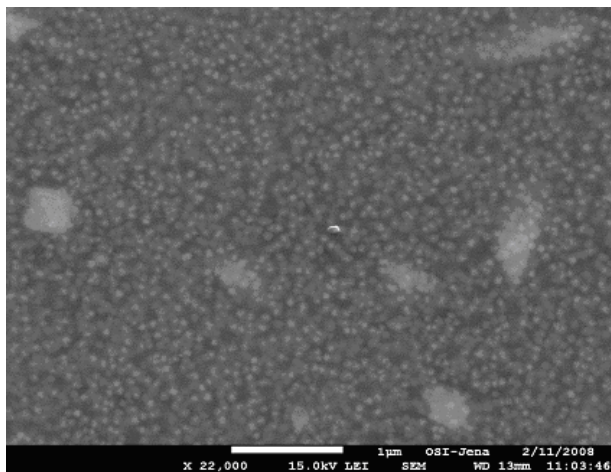


**Fig. 3** SEM (SE) image of C-covered sample A, annealed for 24 h at 600°C – uniform distribution of (Fe, Mn)-based nanocrystals and formation of a second crystalline phase which corresponds to the large ellipsoidal crystals

The data are shown in Fig. 5. Here the hollow symbols represent data for the mean size obtained by SEM images processing. The solid square symbols are taken from [29] and are obtained by anomalous small-angle X-ray scattering (ASAXS) experiments. It is seen in Fig. 5 that the size of the crystals varies from about  $14 \pm 0.5$  nm, [29] to  $50 \pm 1$  nm for annealing times from 40 min to 24 h, respectively. After annealing for 3h at 550°C the size of the precipitated spinel nanocrystals does not change with further increase of the annealing time, i.e. the crystal growth may be supposed to be kinetically self-constrained.

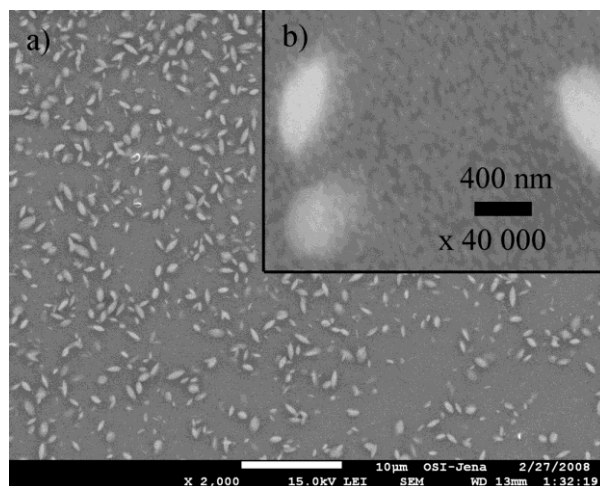


**Fig. 4a and 4b** SEM (SE) images of C-covered sample B, crystallized for 12 h at 600°C – two morphologically different types of crystals, the nanosized (Fe, Mn)-based crystals and elongated  $\text{NaFe}(\text{SiO}_3)_2$ , are present

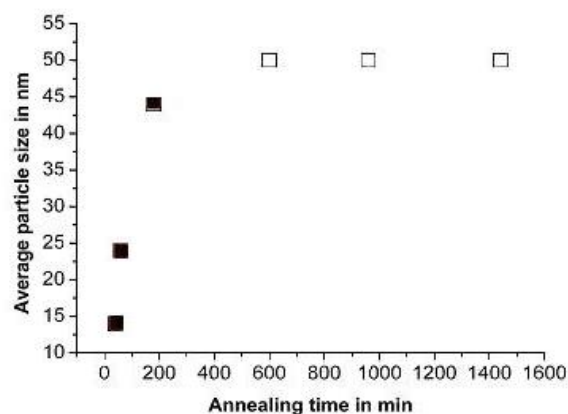


**Fig. 5** Kinetics of crystallization of samples of type A, annealed at 550°C for different times – solid symbols represent ASAXS data taken from [29] and hollow ones are from processing of SEM images

The magnetic properties of selected bulk samples from type A annealed for different times at different temperatures above the glass transition temperature are measured on a vibrating sample magnetometer. As an example, Fig. 6 shows the magnetisation curve of glass A heat-treated for 24 h at 600°C. The nanosized spinel crystals found in this sample display superparamagnetic behavior while the larger aegirine crystals are paramagnetic at room temperature and do not influence the results of the magnetic measurements.

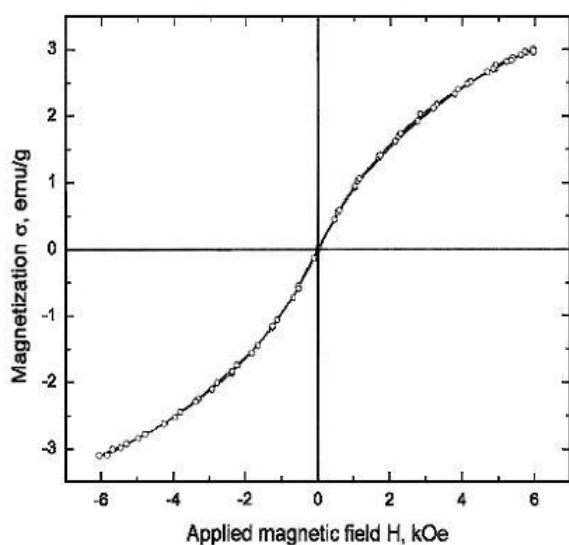


**Fig. 6** Magnetization *versus* intensity of an external magnetic field for a sample A annealed for 24 h at 600°C – superparamagnetic-like behaviour observed

### 3.2 DISCUSSION

The different crystallization behaviour of the oxidized sample B and the reduced sample A could be attributed to the different incorporations of  $\text{Fe}^{2+}$  and  $\text{Fe}^{3+}$  ions in the glass-network, as observed for  $\text{Fe}_2\text{O}_3$  concentrations  $\leq 2$  mol%, [30-40] and is already pointed out and discussed in [25, 29]. The ability to form glasses might also be affected by the redox ratio  $\text{Fe}^{2+}/\text{Fe}^{3+}$  which is supposed to be different in the oxidized and reduced samples. Sample A has a higher  $\text{SiO}_2$  concentration and a lower alkali concentration and is thus assigned a higher acidity of the glass-matrix, according to the acidity-basicity concept, [32, 37]. At the same time, the oxidized sample B has a higher  $\text{Na}_2\text{O}$  concentration and a lower  $\text{SiO}_2$  content, i.e. higher basicity. This determines the higher concentration of  $\text{Fe}^{3+}$  ions in comparison to the concentration of  $\text{Fe}^{2+}$  ones, as suggested by Duffy [32]. The latter implies that crystallization of phases containing mainly ferric ions should be easier in the annealed samples B, which is supported by Figs. 1a and 1b, where the aegirine phase appears at lower annealing times in sample B compared to sample A. For the formation of  $\text{MnFe}_2\text{O}_4$  or rather a mixed spinel phase of the type  $(\text{Fe}^{2+}, \text{Mn}^{2+})(\text{Fe}^{3+}, \text{Mn}^{3+})_2\text{O}_4$ , (as already suggested in Ref. [19]), the valence state in which Mn occurs in the glass is of great importance. In the case of Mn containing oxide glasses, similar redox equilibrium to that described above for Fe is also formed and was already discussed in our previous work, [29]. Thus, the addition of both Mn and Fe oxides enables the

crystallization of a spinel phase from the type  $(\text{Fe}^{2+}, \text{Mn}^{2+})(\text{Fe}^{3+}, \text{Mn}^{3+})_2\text{O}_4$ . The data from Figs. 1 to 4 show that the addition of reducing agents does not change the type of the crystallizing spinel species. It, however, affects the crystallization of the  $\text{NaFe}(\text{SiO}_3)_2$  (aegirine) phase. For the crystallized samples B, the formation of aegirine is observed in larger amounts and for smaller annealing times in comparison to the samples A. The latter can be explained by the higher concentration of  $\text{Fe}^{3+}$ -ions in the case of B. Actually, as shown in Figs. 3 and 4, in the sample B, annealed for 12 h at 600°C, nanocrystals of the (Fe,Mn)-spinel and aegirine crystals of oval shape are present in notable quantities, while in the A type sample crystallized for 24 h at 600°C the same phases but in smaller quantities are found. So, it may be suggested that in the annealed samples A, where the  $\text{SiO}_2$  concentration and hence, the  $\text{Fe}^{2+}/\text{Fe}^{3+}$ -ratio is larger, the formation and the crystal growth of aegirine are suppressed for temperatures up to 600°C and annealing times up to 16 h, (see Figs. 1, 3 and 4).

The average particle sizes, as recently determined from SEM images and SAXS [29] and seen here in Fig. 5, are in the range from 14 to 50 nm and do not change if the annealing time is longer than 3 h. It is suggested in [29] that only the volume fraction of the nano-sized crystalline phase increases while increasing the annealing temperature, which can further have impact on the magnetic properties of the annealed samples [10]. This type of crystallization kinetics shows that the growth of the spinel phase in the reduced samples A is kinetically self-constrained, cf. Fig. 5 and [10, 11, 41, 42]. As described in [29], during the annealing process, the concentration of Fe and Mn ions decreases in vicinity of the growing spinel crystal. So, a silica-rich shell with rapidly increasing viscosity is formed around the growing Fe, Mn-based crystals. When the glass transition temperature of this shell approaches the annealing temperature the crystal growth is decelerated and finally stops for kinetic reasons.

The magnetic measurements show paramagnetic behaviour and absence of hysteresis for the sample of type A, annealed for 3h at 540°C, though in this sample nanocrystals are contained. The reason for this magnetic behaviour is not clear and needs further investigation. In contrast to the paramagnetic behaviour of the sample annealed for 3 h at 540°C, the sample, crystallized for 24 h at 600°C, possesses superparamagnetic properties at room temperature and no hysteresis – as seen in Fig. 6. The same is already observed in other glass-

ceramic systems containing nanosized spinel crystals [10, 15]. However, here, due to lower intensities of the applied external magnetic field as compared to the data in [10], we suppose that no saturation of the mass magnetization is reached. So, further investigation is needed in this direction in order to better elucidate the magnetic behaviour of the studied glass-ceramic materials.

#### 4. CONCLUSION

Crystalline spinel phase of the type  $(\text{Mn}^{2+}, \text{Fe}^{2+})(\text{Fe}^{3+}, \text{Mn}^{3+})_2\text{O}_4$  is precipitated in the two investigated compositions with 15 mol% Fe-oxide for temperatures up to 600°C, while for longer annealing times at 600°C a second crystalline phase – aegirine,  $\text{NaFe}(\text{SiO}_3)_2$  – is also formed. The precipitation of hematite is avoided in the whole temperature interval investigated for both reduced and oxidized compositions. For crystallization times from 40 min to 24 h and annealing temperature of 550°C, kinetically self-constrained growth of the spinel nanocrystals is observed, with average crystallite sizes of about 50 nm which does not further increase for times longer than 3 h. The magnetic measurements on a sample annealed for 24h at 600°C show superparamagnetic behaviour at room temperature.

**Acknowledgements:** *The present work was partially supported by contract 10–929/2011 of the University of Chemical Technology and Metallurgy. The authors would also like to thank Prof. M. Mikhov from the Physics Faculty of Sofia University for performing the magnetic measurements.*

#### REFERENCES:

- 1 A.Karamanov, M.Pelino, *J. Non-Cryst. Sol.* **281** 139 (2001).
- 2 M.Romero, J.M.Rincon, *J. Am. Ceram. Soc.* **82** 1313 (1999).
- 3 J.D.Mackenzie, *J. Non-Cryst. Sol.* **2** 16 (1970).
- 4 L.Murawski, C.H.Chung, J.D.Mackenzie, *J. Non-Cryst. Sol.* **32** 91 (1979).
- 5 J.D.Mackenzie, *J. Am. Ceram. Soc.* **47** 211 (1964).
- 6 J.D.Mackenzie *in: Modern Aspects of the Vitreous State*, vol. 3, J.D. Mackenzie (Ed.), Butterworths, London, 1964, p. 126.
- 7 H.J.L. Trap, J.M.Stevens, *Phys. Chem. Glasses* **4** 193 (1963).
- 8 R.A.Anderson, R.K.MacCrone, *J. Non-Cryst. Sol.* **14** 112 (1974).
- 9 J.Allersma, J.D.Mackenzie, *J. Chem. Phys.* **47** 1406 (1967).
- 10 S.Woltz, R.Hiergeist, P.Görnert, C.Rüssel, *J. Magn. Mater.* **298** 7 (2006).
- 11 S.Woltz, C.Rüssel, *J. Non-Cryst. Sol.* **337** 226 (2004).
- 12 H.H.Qiu, M.Kudo, H.Sakata, *Mater. Chem. Phys.* **51** 233 (1997).
- 13 H.H.Qiu, H.Mori, H. Sakata, T.Hirayama, *J. Ceram. Soc. Jpn.* **103** 32 (1995).
- 14 S.Roy, D.Chakravorty, *J. Mater. Res.* **9** 2314 (1994).
- 15 S.Odenbach, *J. Phys: Condens. Matter.* **16** 1135 (2004).
- 16 G.Y.Zhou, Z.Y.Jiang, *Smart Mater. Struct.* **13** 309 (2004).
- 17 Y.Sakai, N.Abe, S.Takeuchi, F.Takahashi, *J. Ferment. Bioeng.* **80**: 300 (1995).
- 18 T.Aytur, J.Foley, M.Anwar, B.Boser, E.Harris, P.R.Beatty, *J. Immunol. Methods* **314** 21 (2006).
- 19 Z.J.Zhang, Z.L.Wang, B.C. Chakoumakos, J.S. Yin, *J. Am. Chem. Soc.* **120** 1800 (1998).
- 20 X.Wang, Y.Li, *Chem. Commun.* 2901 (2007), DOI: 10.1039/b700183e.
- 21 H.Si, C.Zhou, H.Wang, S.Lou, S.Li, Z.Lu, L.S.Li, *J. Coll. Interf. Sci.* **327** 466 (2008).
- 22 W.Shi, N.Chopra, *J Nanopart. Res.* (2010), DOI: 10.1007/s11051-010-0086-0.
- 23 T.Herranz, S.Rojas, M.Ojeda, F.J.Perez-Alonso, P.Terrerros, K.Pirota, J.L.G.Fierro, *Chem. Mater.* **18** 2364 (2006).
- 24 R.Harizanova, G.Völksch, C.Rüssel, *J. Mater. Sci.* **45** 1350 (2010).
- 25 R.Harizanova, G.Völksch, C.Rüssel, *Mater. Res. Bull.* (2010), doi:10.1016/j.materresbull.2010.09.036.
- 26 G.Völksch, R.Harizanova, C.Rüssel, S.Mitsche, P.Pöhl, *Glastech. Ber. Glass Sci. Technol.* **77C** 438 (2004).
- 27 R.Harizanova, R.Keding, C.Rüssel, *J. Non-Cryst. Sol.* **354** 65 (2008).
- 28 R.Harizanova, R.Keding, G.Völksch, C.Rüssel, *Eur. J. Glass Sci. Technol. B* **49** 177 (2008).
- 29 R.Harizanova, I.Gugov, C.Rüssel, D.Tatchev, V.S.Raghuwanshi, A.Hoell, *J. Mater. Sci.* (2011), DOI 10.1007/s10853-011-5840-x.
- 30 C.Rüssel, A.Wiedenroth, *Chem. Geol.* **213** 125 (2004).
- 31 R.A.Levy, C.H.Lupis, P.A.Flinn, *Phys. Chem. Glasses* **17** 94 (1976).
- 32 A.Duffy, *Phys. Chem. Glasses* **40** 54 (1999).
- 33 A.Wiedenroth, C.Rüssel, *J. Non-Cryst. Sol.* **347** 180 (2004).
- 34 A.Wiedenroth, C.Rüssel, *J. Non-Cryst. Sol.* **297** 173 (2002).
- 35 G.Gravanis, C.Rüssel, *Glastech. Ber.* **62** 345 (1989).
- 36 P.A.Bingham, J.M.Parker, T.Searle, J.M.Williams, K.Fyles, *J. Non-Cryst. Sol.* **253** 203 (1999).
- 37 J.A.Duffy, M.D.Ingram, *J. Non-Cryst. Sol.* **21** 373 (1976).

- 38 L.D.Pye, A.Montenero, I.Joseph (Eds.), *Properties of Glass-Forming Melts*, Taylor & Francis, Boca Raton, 2005, p. 27.
- 39 L.Kido, M.Müller, C.Rüssel, *Chem. Mater.* **17** 3929 (2005).
- 40 L.Kido, M.Müller, C.Rüssel, *J. Non-Cryst. Sol.* **351** 523 (2005).
- 41 C.Rüssel, *Chem.Mater.* **17** 5843 (2005).
- 42 C. Bocker, C.Rüssel, *J. Europ. Ceram. Soc.* **29** 1221 (2009).

## КРИСТАЛИЗАЦИОННО ПОВЕДЕНИЕ И МАГНИТНИ СВОЙСТВА НА НАТРИЕВО-СИЛИКАТНИ СЪТЪКЛА, СЪДЪРЖАЩИ ОКСИДИ НА ЖЕЛЯЗОТО И МАНГАНА

<sup>1</sup>Р. Харизанова, <sup>1</sup>И.Гугов, <sup>2</sup>К. Рюсел

<sup>1</sup>Химикотехнологичен и Металургичен университет, бул. "Кл. Охридски" № 8, 1756, София, България  
<sup>2</sup>Ото Шот институт, Фридрих Шилер университет, ул. "Фраунхофер" №. 6, 07743, Йена, Германия

Постъпила на 24 януари, 2012 г.; коригирана на 5 март, 2012 г.

(Резюме)

Оксидните стъкла и нанокристални стъклокерамики, съдържащи йони на преходните метали с висока концентрация, проявяват авангардни и необичайни електрични и магнитни свойства и намират разнообразни приложения в магнитореологията, електрониката, магниторезонансните изследвания и сензорните технологии. Настоящата работа е посветена на изучаването на кристализационното поведение, фазообразуването и магнитните свойства на продуктите на синтез в системата  $\text{Na}_2\text{O}/\text{MnO}/\text{SiO}_2/\text{Fe}_2\text{O}_3$ . Синтезирани са две стъкла с 15 мол %  $\text{Fe}_2\text{O}_3$  и различна концентрация на  $\text{MnO}$ , стопени при окислителни или редуциращи условия. Впоследствие стъклата са темперирани чрез прилагане на различни програми температура-време, целящи получаването на наноразмерни магнитни кристали. Фазовият състав и микроструктурата на стъклокерamikите са изучени с използване на рентгенова дифракция и електронна микроскопия. Получените данни са използвани за изследване на кинетиката на кристализация. Магнитните свойства на избрани проби, измерени с използване на вибрационна магнитометрия, варират от пара- до суперпарамагнитни.